

EFFECTS OF ELECTRONS, PROTONS, AND ULTRAVIOLET RADIATION ON THERMOPHYSICAL PROPERTIES OF POLYMERIC FILMS

Dennis A. Russell*, John W. Connell†, Lawrence B. Fogdall‡, Werner W. Winkler§

ABSTRACT

The response of coated thin polymer films to ultraviolet (UV), electron and proton radiation simultaneously has been evaluated, with selected measurements *in situ*. Exposure was intended to simulate the electron and proton radiation environment near the Earth-Sun Lagrangian points (L1 and L2) for five years and ~1000 equivalent solar hours (ESH) UV. These orbital environments are relevant to several potential missions such as the Next Generation Space Telescope and Geomagnetic Storm Warning, both of which may use thin film based structures for a sunshade and solar sail, respectively. The thin film candidates (12.5 μm thick) consisted of commercially available materials (Kapton® E, HN, Upilex® S, CP-1, CP-2, TOR-RC and TOR-LMBP) that were metalized on one side with vapor deposited aluminum. All of the films are aromatic polyimides, with the exception of TOR-LMBP, which is a copoly(arylene ether benzimidazole). The films were exposed as second surface mirrors and the effects of the exposure on solar absorptance (α), thermal emittance (ϵ) and tensile properties were determined. The *in situ* changes in solar absorptance from Kapton® and Upilex® were less than 0.1, whereas the solar absorptance of TOR and CP films increased by more than 0.3 without saturating. The thermal emittance measurements also showed that the Kapton® and Upilex® materials increased only 1-2%, but the remaining materials increased 5-8%. Based on tensile property measurements made in air following the test, the failure stress of every type of polymer film decreased as a result of irradiation. The polymers most stable in reflectance, namely Upilex® and Kapton®, were also the strongest in tension before irradiation, and they retained the greatest percentage of tensile strength. The films less stable in reflectance were also weaker in tension, and lost more tensile strength as a result of irradiation. The apparent failure strain (as a percent of original gage length) of every type of polymer film except TOR-RC, decreased as a result of irradiation.

INTRODUCTION

Significant attention has recently been given to the concept of using lightweight, compliant structures that can be folded into the compact volumes of conventional launch vehicles and subsequently deployed on orbit as a means to achieve very large structures in space, hence the term Gossamer structures. Relative to on-orbit construction this approach can offer significant reductions in cost, complexity and risk to astronauts. These structural concepts typically are comprised of a support structure that can be deployed via mechanical, inflatable or other means and subsequently rigidized; and a thin film that serves as an antenna, sail, reflector, concentrator, sunshade, etc. Recent demonstrations of large deployable/inflatable film-based space structures such as a 20 m solar sail (Znamya-2, "New Light") and a 14 m lenticular inflatable antenna have provided glimpses into future possibilities for Gossamer spacecraft. Consequently, a significant number of future missions utilizing Gossamer spacecraft concepts have been proposed by the National Aeronautics and Space Administration (NASA), Department of Defense (DOD), other United States Government and foreign space agencies.

Materials are one of many technologies that must come together in an integrated fashion to successfully advance the Gossamer spacecraft concept to realization. Materials are enabling for both the support structure and the film portion of Gossamer spacecraft. They must have specific combinations of properties, and maintain these properties over the life of the mission. The property requirements can vary significantly, depending upon the mission and space environment.

Earlier programs and space flights have laid a good foundation for materials now being developed. Polyimides, polyesters, and perfluorinated ethylene-propylene copolymers have been used extensively on spacecraft designed for a wide range of environmental exposure levels. Some copolymers have been reasonably stable in reflectance when exposed to UV near one astronomical unit (AU). However, they lose significant

Copyright © 2001 by The Boeing Co.
Published by the American Institute of
Aeronautics and Astronautics, Inc.,
with permission.

*Boeing Phantom Works, Seattle WA 98124-3999

†NASA-Langley Research Center, Hampton VA 23681-0001

‡Light Technologies, Inc., Seattle WA 98112-2906. Member AIAA

§Formerly of the German Space Agency; Sankt Augustin, Germany

amounts of reflectance, and change reflective character if exposed to electrons at fluxes near the peak rates measured at synchronous altitudes. Electrons typically cause a bulk effect, with the polymer becoming a light-scattering medium.¹ Polyimide films such as Kapton® have performed well in space, and have survived well in simulations of low-energy protons such as the 1-10 keV solar wind. However, they have degraded heavily at high proton fluences, or when exposed to UV at intensities representative of near-Sun missions, unless protectively overcoated.² The U.S.-German HELIOS spacecraft survived thermal loading up to ~10 Suns for several years with metalized polymer films and other advanced technologies including control of electrical conductivity systemwide.³ The HELIOS program studied gossamer films. Poly(paraxylylene) supported in a stainless steel mesh (a potential weight penalty) performed marginally, but bonded Al₂O₃/Al-overcoated quarter-mil Kapton® was stable even at accelerated simulation intensities. The latest generation of materials includes self-supporting films having ~13 micrometer (0.5-mil) thickness. Boeing's irradiation of samples of these materials has been documented for NASA,⁴ and is the subject of this paper.

EXPERIMENTAL APPROACH

Radiation Environment

It was the goal of the program to provide a 5-year simulation of two regions of space, the environment at 0.98 astronomical units (AU) where the Geostorm satellite will orbit, and the environment at the second Lagrangian point (L2) where the Next Generation Space Telescope (NGST) will be positioned. The Geostorm location between the Sun and the Earth is far beyond the influence of the Earth's magnetic field, making the environment of interest that of the solar wind and solar events. The L2 position, on the other hand, is located on the far side of the Earth away from the Sun. At this position, a spacecraft would pass through the Earth's geotail created by the interaction of the geomagnetic field with the solar wind. The best estimate available for the radiation environment was arrived upon by researching available information and by discussions with experts from NASA, academia and industry. The levels present in these regions are continually being refined; however, it is understood that by far the major contribution to both environments was the solar wind.

The electron and proton fluence levels were determined by first generating a dose depth profile of a representative material (Kapton in this case) for the solar wind at L1. The goal then is to best approximate this profile with the beam energies available in the chamber. This was accomplished by generating a test protocol that used 40-keV protons with a range of 0.52

micrometers (0.02 mils) to deliver the very high dose indicated near the surface. Electrons of 40-keV energy with a much deeper dose depth profile were used to deliver the bulk dose.

Exposure Facilities

Boeing's Combined Radiation Effects Test Chamber (CRETC), diagramed in Figure 1, provided the appropriate experiment environment. The chamber is equipped with sources for both a 10 to 50 kV rastered proton beam and a 30 to 60 kV electron beam. A water-cooled 6000 watt Xenon arc lamp provides continuum ultraviolet exposure from 200 to 400 μm at an intensity of 1-3 UV suns. The clean, cryo-pumped chamber is also fitted with a spectrophotometer that enabled *in situ* reflectance measurements to be made periodically throughout exposures. It is not necessary to remove the samples from the sample holder or the vacuum to make the reflectance measurements.

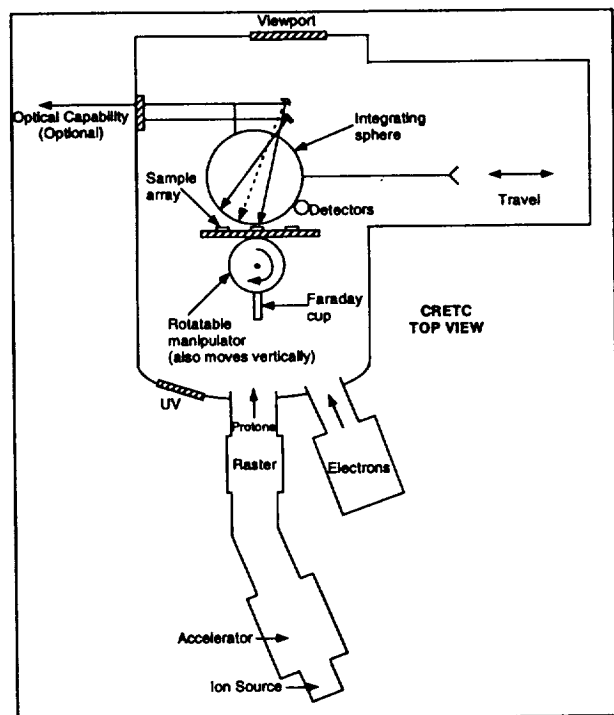


Figure 1 CRETC Chamber Layout

The UV intensity was measured across the overall beam-space that the specimen array occupied and was within ± 10 percent when using approximately 1.5 UV suns. (One total sun is approximately 0.135 watt/cm²; the sun's UV content is approximately 9.1% of its overall output, for a value of approximately 0.012 watt/cm²/UV-sun.) The areas of lowest UV intensity are small portions of the four corners of the array-space.

Characteristics of the proton and electron beams were determined with Faraday cups that track the

chamber horizontal and vertical centerlines (bisecting the array of specimens). It was determined that the 40-keV electrons were quite uniform to $\pm 5\%$. The 40-keV proton beam, which is rastered with significant overlaps to provide uniformity along with a larger beam size, was uniform to ± 15 percent over the sample array.

Test Specimen and Fixture

NASA Langley Research Center provided the test specimens consisting of 7 types, commercially available Kapton® E and HN, Upilex® S, CP-1 and CP-2⁵ and 2 experimental films TOR-RC and TOR-LMBP⁶. Kapton® and Upilex® are mature film products that have been optimized for thermal and mechanical properties through synthesis and processing. Consequently, they exhibit significantly higher strengths, moduli and strain to failures than the batch cast experimental films.

The exposure area of the CRETC allowed for a total of 15 specimens. The minimum area required for the emittance measurement and the maximum exposure area determined the number of specimens. In addition, the tensile strength measurements required a length of unexposed material at each end. Therefore a custom test fixture sized for specimens approximately 75 mm (3 inches) long and 16 mm (0.65 inch) wide, with a central exposure and measurement section of 20 mm (0.8 inch) long was designed.

Each row of specimens was mounted to a slightly curved shape mandrel-like bar that secures each test specimen in place during exposure. Figure 2 is an "exploded" view of the fixture. Each specimen was secured from the end on the backside of the fixture. One feature of the fixture was a thin shield between the rows of test specimens, to provide for a well-defined central irradiation section.

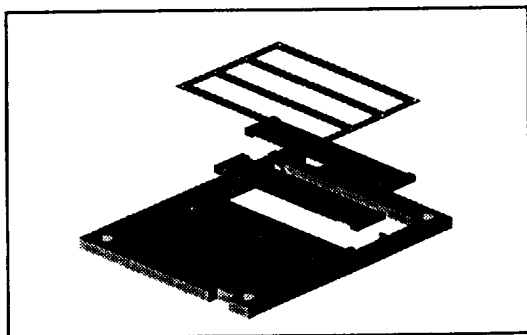


Figure 2 Exploded View of Specimen Fixture

Specimen Preparation and Mounting

The thin films (12.5 mm thick) were difficult to handle. A cutting template tool was machined to aid in cutting the specimens from the larger sheets provided

by the customer. Microscopy was used to determine machining direction (if applicable) as well as to assure that the films would be exposed as second-surface mirrors. The more fragile experimental polymer films were the most difficult to cut. Specimens that developed ragged edges or tears were not used in the irradiations, but were set aside as extra controls.

The fabricated test fixture was wiped with isopropyl alcohol, then ultrasonically cleaned in a detergent wash and rinse, and finally given an ethanol solvent rinse and dry.

Sample integration was performed using cleanroom gloves inside a clean laminar flow bench. The first step of the integration was to attach the cut specimens to their holding bars (each bar is described elsewhere as like a section of a very slightly curved mandrel). Small pieces of Kapton tape were used as needed to aid the initial securing of specimen ends behind their hold-down metal strips. One at a time, each specimen was then wrapped "down" and over the front surface of its mandrel, then looped over the top and back of the mandrel, whereupon small weights were attached to each sample's bottom grip area, to keep each specimen in mild tensile stress, but with freedom to shrink or elongate in response to radiation. The front cover shield was then attached, to define the overall exposure area of each specimen exactly. The result was an array of 5 samples in each of 3 horizontal rows on mandrel bars.

Property Measurement

Reflectance. The Boeing CRETC has a double-beam spectrophotometer that is optically coupled to the locations of test samples in the vacuum chamber (Figure 1). With appropriate measuring light sources (UV to near-IR), and with light detectors *in situ*, the value of a test surface's spectral reflectance, as modified by radiation or perhaps other stresses, is determined during measurements and retained for computer analysis. In Boeing's facility, an integrating sphere in the test chamber, between the detector and a sample being measured, produces a measurement of hemispherical reflectance. The spectral range is 250 nm to about 2500 nm. A sample is illuminated spectrally since the spectrophotometer optical path includes the monochromator after the light source(s). The spectral illumination begins with longest wavelength light (lowest eV value), and the measurement proceeds to shorter wavelengths. This is a non-destructive measurement. With opaque samples, solar absorptance is derived by simple subtraction (using the appropriate solar wavelength weighting).

Emittance. A non-destructive measurement using near-infrared radiation can be given to a film sample by laying it over an aperture provided in a Gier-Dunkle

Emittance Inspection Device (DB100). Boeing performed a series of these room temperature measurements as part of this program, in air following the *in situ* irradiation. A number of unirradiated samples cut from the same polymer sheets, were used as unexposed comparison samples so all specimens were measured in the same run. The measuring device illuminates each sample with polychromatic radiation, and the apparatus circuitry computes a weighted infrared reflectance value internally. With opaque specimens as in this program, the values of thermal emittance coefficients were derived by simple subtraction from the measured reflectance values.

Tensile. After completion of the emittance measurements on all exposed samples as well as on selected "comparison" or unexposed samples, mechanical property measurements were made. The test machine used for the property testing was a MII-50 UD Satec universal test machine with a 440-kg (1000-pound) load cell. The cell is calibrated down to 2 pounds with a resolution down to 0.001 pounds. Instron hydraulic grips with rubber pads were used to clamp each test film in turn. All measurements were made at room temperature.

EXPERIMENTAL DATA

Exposure Summary

The simultaneous exposure of protons, electrons and UV simulating a 5-year (60-month) mission at L1/L2 was divided into 5 exposure segments. Table 1 lists the proton and electron fluences and the equivalent UV exposure hours for each segment. While the total proton and electron fluences simulated the entire 60-month mission it was not possible to provide a UV exposure that simulated the full mission within the scope of the contract. Therefore, the highest amount of UV exposure possible was accumulated as dictated by the exposure times of the protons and electrons.

Table 1 Exposure Summary

| Exposure Segments | Equivalent Mission Duration (months) | Proton Fluence (p/cm ²) | Electron Fluence (e/cm ²) | UV Exposure (hours) |
|-------------------|--------------------------------------|-------------------------------------|---------------------------------------|---------------------|
| 1 | ~3 | 3.6E+13 | 5.0E+14 | 90 |
| 2 | 12 | 2.0E+14 | 1.6E+15 | 330 |
| 3 | 24 | 3.9E+14 | 3.2E+15 | 480 |
| 4 | 42 | 7.1E+14 | 5.7E+15 | 685 |
| 5 | 60 | 1.0E+15 | 8.0E+15 | 1000 |

The average flux over the entire exposure period was 4.8E8 p/cm²-s, 3.9E9 e/cm²-s and 1.5 equivalent UV suns. The chamber vacuum pressure level began at 9E-7 at the start of the exposure and quickly leveled out at 2E-7 torr. The CRETC exposure systems are designed to operate continuously except for brief periods each day devoted to dosimetry and cleaning of the UV source. The exposure was also interrupted during scheduled reflectance measurements.

Solar Absorptance

The solar absorptance values were calculated from the spectral reflectance data measured by the spectrophotometer. From the 240 specific wavelengths available from each data set, 100 wavelengths representing the relative spectral weighting of the Sun's radiance curve were used in the calculation of solar absorptance. As the exposure continued the TOR-LMBP sample type started to tear and by the third measurement level both specimens had torn and were unmeasurable. Table 2 lists all the individual values and Figure 3 plots the average increase in the solar absorptance for each specimen type as a function of the exposure.

Thermal Emittance

The emittance results for both the unexposed and exposed samples were calculated from the measured reflectance values by subtraction for these opaque materials. The bar graph in Figure 4 gives a quick visual summary of the results.

Tensile Properties

Sixteen specimens failed in the gage section and nineteen failed in one or the other grip areas. In general, the values for failure strain in the case of grip failures were similar to the values obtained for the cases of gage failures. Figures 5, 6, and 7 summarize the results in bar graph format.

The apparent modulus values were not affected appreciably by the radiation exposure. However, the failure stress and strain were generally affected. Several exceptions include TOR-RC's failure strain values, which were very low to begin with, remained low; and stress at failure for Upilex®S showed a decrease in only one of the two samples. These remarks illustrate that the small number of exposed samples available combined with the difficulty of making this type of measurement on very thin films reduces the usefulness of the results to primarily indicating trends.

Table 2 Individual Specimen *In Situ* Solar Absorptance Values

| Exposure Segment | | 0 | 1 | 2 | 3 | 4 | 5 |
|------------------|-----------------|---------------------|--------|--------|--------|--------|--------|
| Sample Material | Exposure Levels | 0 p/cm ² | 3.6E13 | 2.0E14 | 3.9E14 | 7.1E14 | 1.0E15 |
| | | 0 e/cm ² | 5.0E14 | 1.6E15 | 3.2E15 | 5.7E15 | 8.0E15 |
| | ID | 0 hr. UV | 90 | 330 | 480 | 685 | 1000 |
| Kapton® E | 2 | 0.300 | 0.326 | 0.328 | 0.335 | 0.352 | 0.373 |
| | 7 | 0.304 | 0.326 | 0.328 | 0.340 | 0.352 | 0.373 |
| | 15 | 0.304 | 0.329 | 0.330 | 0.346 | 0.356 | 0.375 |
| Kapton® HN | 1 | 0.318 | 0.337 | 0.329 | 0.335 | 0.356 | 0.380 |
| | 8 | 0.314 | 0.339 | 0.337 | 0.349 | 0.365 | 0.389 |
| Upilex® S | 4 | 0.351 | 0.376 | 0.370 | 0.383 | 0.392 | 0.407 |
| | 11 | 0.355 | 0.381 | 0.383 | 0.398 | 0.399 | 0.413 |
| CP-1 | 9 | 0.213 | 0.246 | 0.339 | 0.409 | 0.473 | 0.546 |
| | 14 | 0.217 | 0.238 | 0.316 | 0.382 | 0.441 | 0.491 |
| CP-2 | 3 | 0.215 | 0.241 | 0.315 | 0.376 | 0.432 | 0.484 |
| | 6 | 0.211 | 0.233 | 0.289 | 0.360 | 0.406 | 0.458 |
| TOR-RC | 10 | 0.194 | 0.258 | 0.374 | 0.440 | 0.496 | 0.560 |
| | 13 | 0.193 | 0.246 | 0.365 | 0.421 | 0.478 | 0.536 |
| TOR-LMBP | 5 | 0.233 | 0.252 | | | | |
| | 12 | 0.227 | 0.280 | | | | |

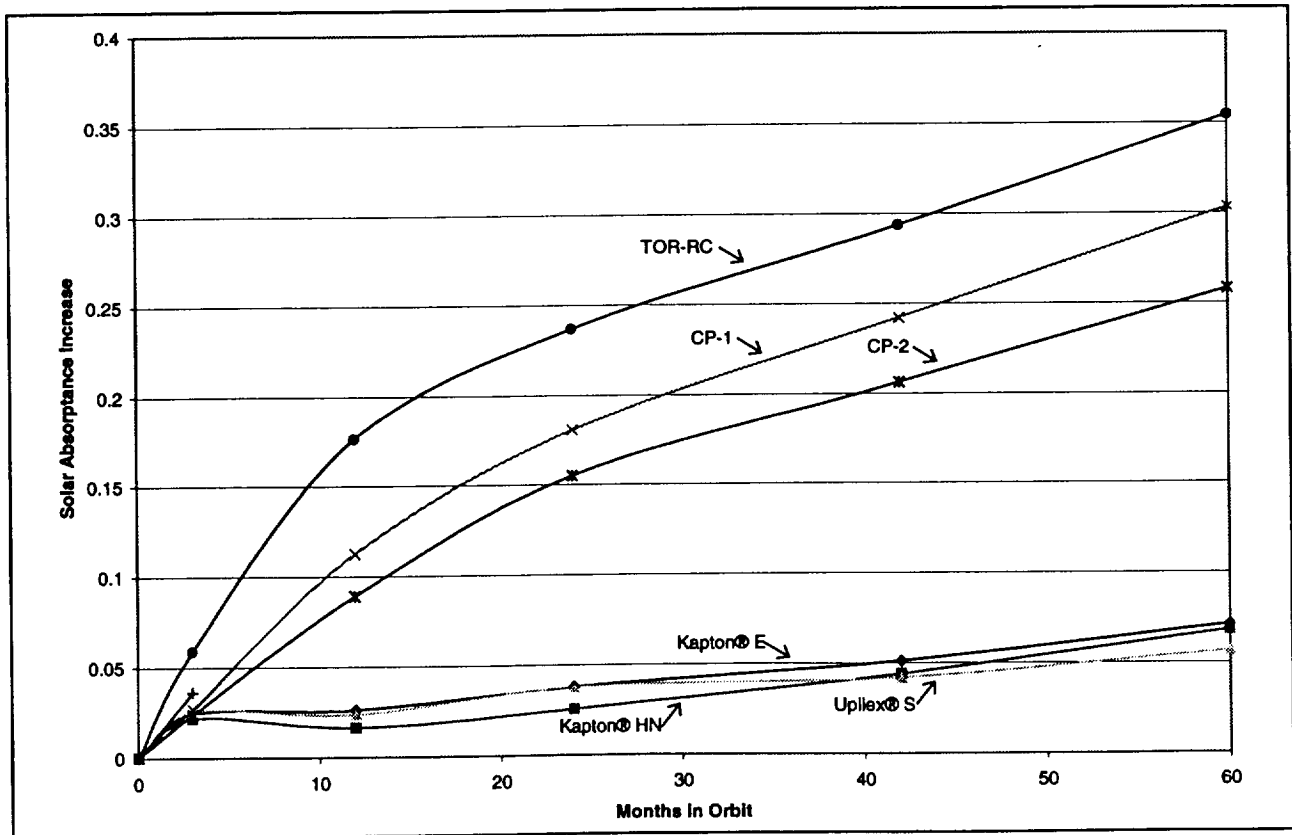


Figure 3 Increase in Solar Absorptance as a function of Exposure

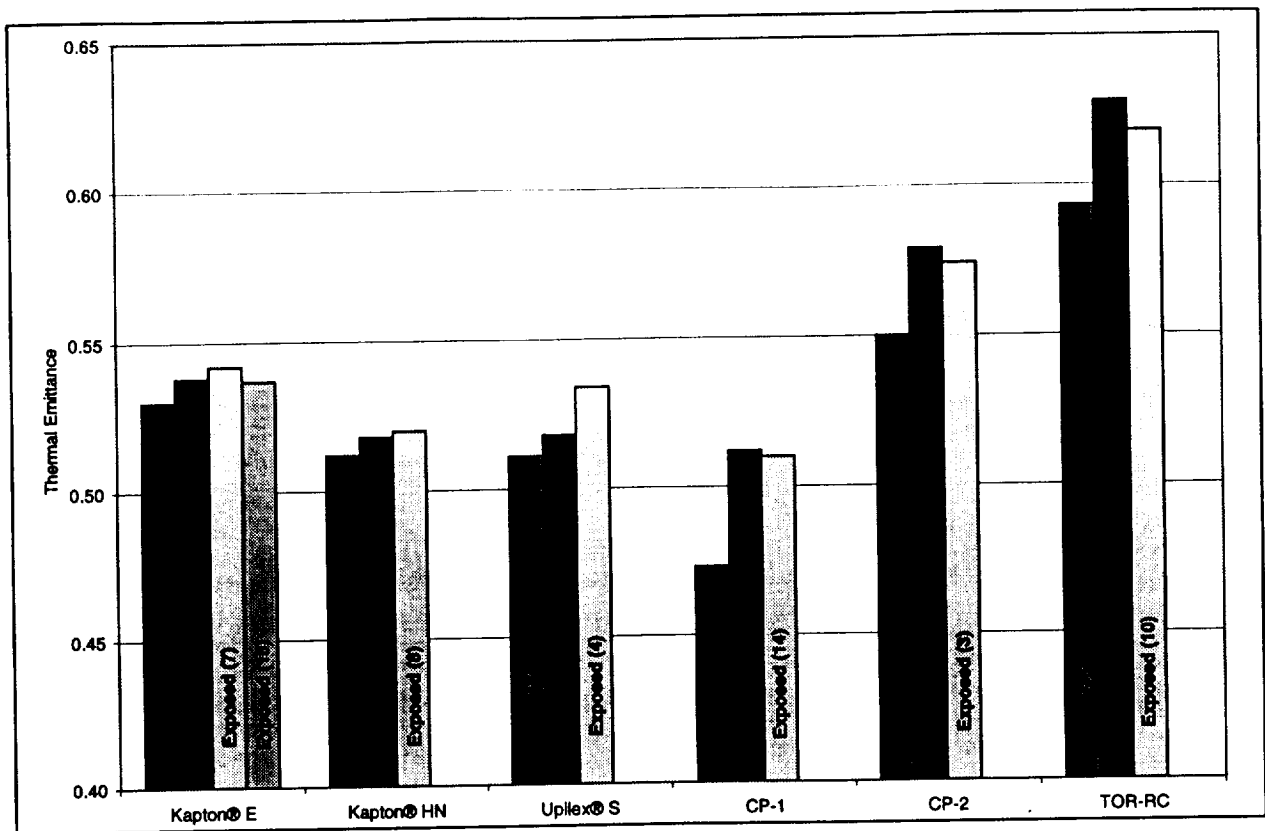


Figure 4 Thermal Emittance

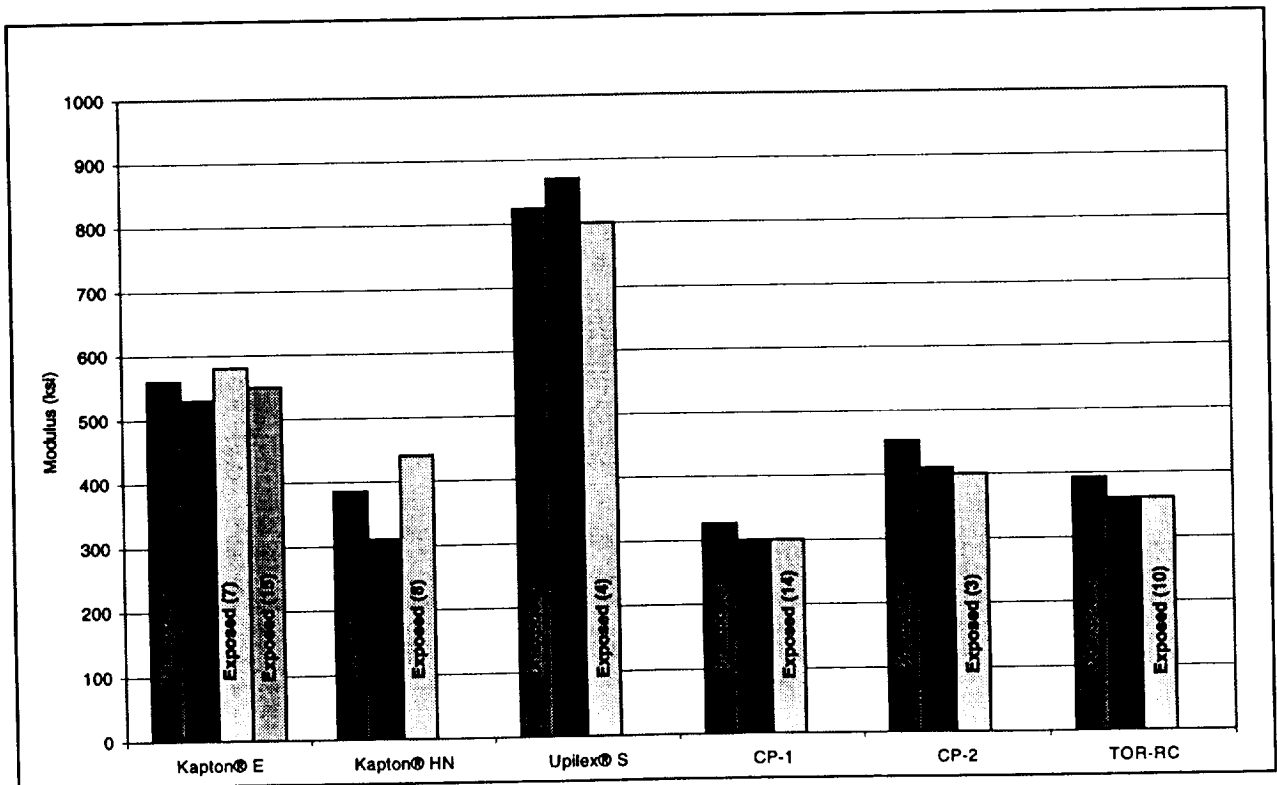


Figure 5 Apparent Modulus

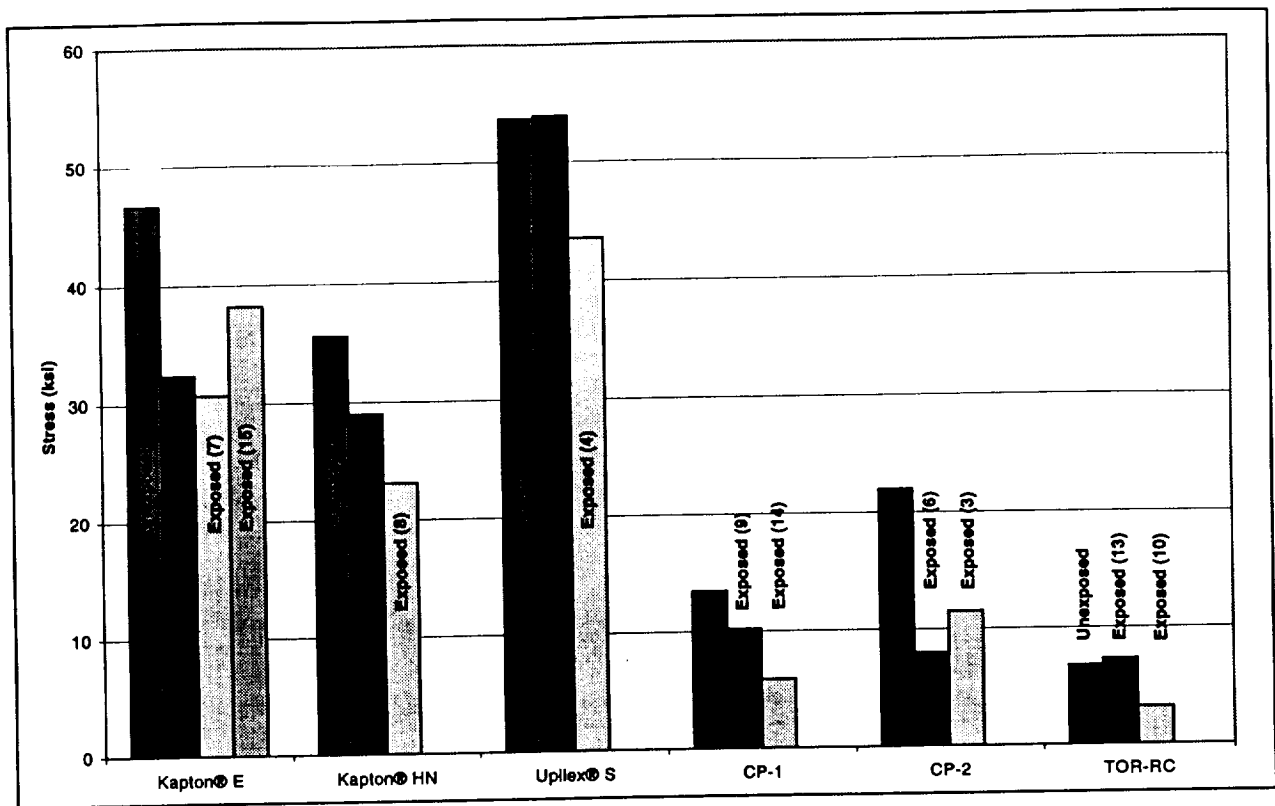


Figure 6 Apparent Failure Stress

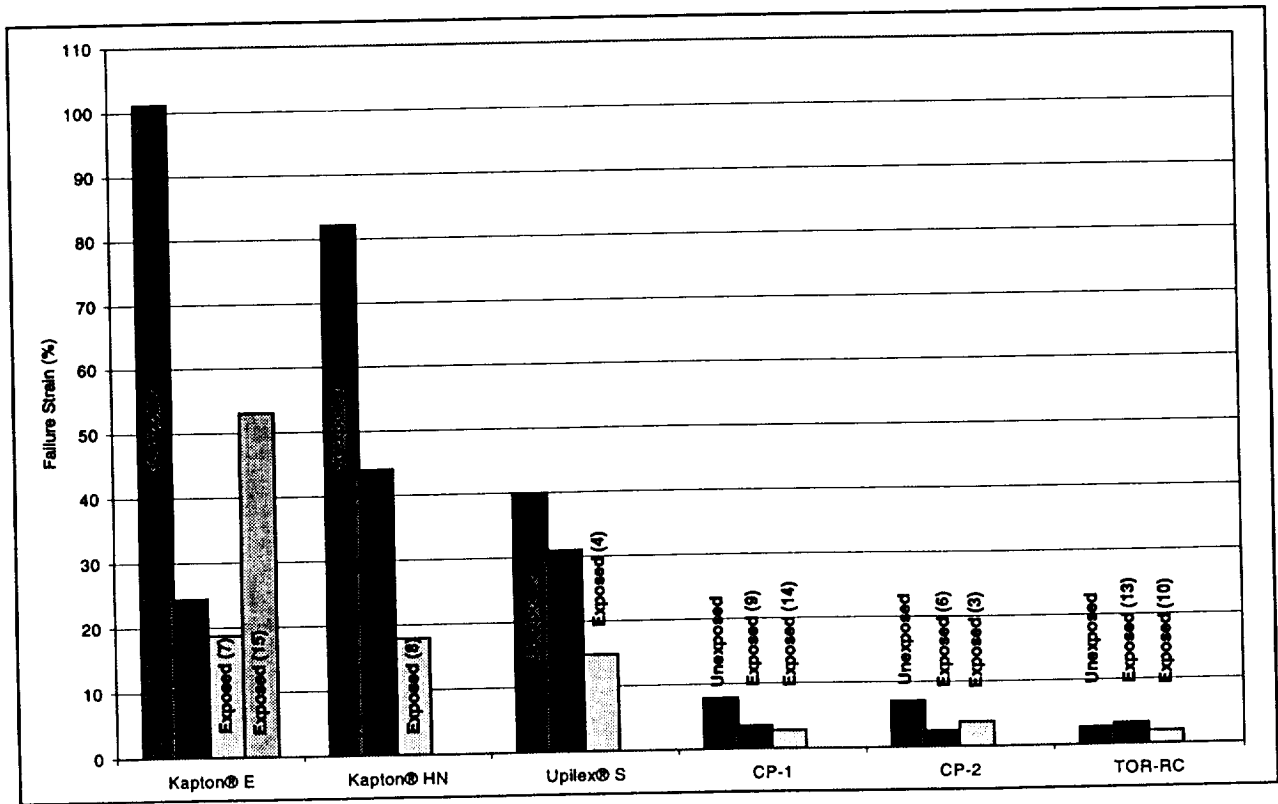


Figure 7 Apparent Failure Strain

DISCUSSION and CONCLUSIONS

Reflectance measured *in situ* was always found to decrease after exposure to simulated space radiation. Thus the computed values of each sample's solar absorptance increased as exposure to radiation continued, to the end of the test without saturation. Certain polymer films that were colorless prior to irradiation became considerably more absorptive, and acquired a "bronze" color, during irradiation. The polymers that originally were colorless, more than doubled their solar absorptance (from about 0.2 to nearly 0.5). On the other hand, Kapton® specimens increased about 0.07 in solar absorptance, from base values of about 0.3. Upilex®S was slightly more stable for solar absorptance, increasing about 0.06 (from base values of about 0.35). TOR-RC nearly tripled in solar absorptance by the end of the test (from base values of approximately 0.2). TOR-LMBP distorted and then disintegrated during the first quarter or so of the test period. Figure 3 summarizes the increase in solar absorptance obtained on each of the irradiated polymer films types. The experimental data divide into two principal groups, one of them having much more stable reflectance than the other does. The changes in solar absorptance from Kapton® and Upilex® samples remain less than 0.1, whereas the solar absorptance changes in TOR and CP film samples increase by more than 0.3 without saturating.

The thermal emittance values measured (in air) on the Kapton® specimens remained essentially unchanged within experimental uncertainty. On the other hand, the emittance of polymer CP-1 increased about eight percent in air (from about 0.47 to about 0.51 decimally) as a result of the combined UV/proton/electron irradiation performed. The emittance of CP-2 and TOR-RC increased perhaps half as much.

Based on tensile property measurements made in air following the test, the failure stress of every type of polymer film decreased as a result of being irradiated. The polymers most stable in reflectance, namely Upilex®S and Kapton®, were also the strongest in tension before irradiation, and they retained the greatest percentage tensile strength. The films less stable in reflectance were also weaker in tension, and lost more tensile strength as a result of irradiation. This is illustrated in Figure 6. The apparent failure strain (as a percent of original gage length) of every type of polymer film except TOR-RC, decreased as a result of irradiation. The decrease was "dramatic" in Kapton®. Apparent modulus generally decreased so slightly due to irradiation that the changes are not very significant.

No direct measurement of sample temperature was made during the irradiation for this program. However, when preparing the same test fixture for a

recent irradiation of similar materials,⁷ one sample-holding mandrel was machined to place a thermocouple near one corner specimen. The thermocouple was shielded from direct exposure to the simulated Sun source. As in this program, water cooling adjacent to, but thermally decoupled from, the mandrels provided a baseline set of conditions that included a temperature of approximately 19 C for the samples and their mandrels when the chamber interior was dark. Then, under an intensity of approximately 2 UV suns, the mandrel temperature rose about five degrees Celsius (from ~19 C to 24 C or less) within minutes after beginning the exposure of samples to the solar beam.

Further analysis has been done to estimate the temperature of the polymer films themselves during irradiation. The film samples were not bonded to their mandrels. Most samples had the majority of their area in contact with their mandrel. However, some specimens did not hang straight, though weighted. Despite being thin, they were not fully compliant with efforts to have them be draped uniformly around their mandrels. Therefore, portions of those samples did not have total thermal contact with their mandrel surfaces. Those portions of films with no or poor thermal contact would rise to higher values of equilibrium temperature during irradiation, depending on their absorptance and emittance properties, the intensity of the simulated Sun, and the temperature of adjacent radiative surfaces such as the mandrels. Calculations show that detached portions of "low" absorptance films such as the CP series may equilibrate at about 80 C when illuminated by 1.5 suns, but could rise to ~170 C in their degraded states (Table 2 and Figure 3). In contrast, portions of Kapton® and Upilex® samples that are irradiated while detached from cooled substrates would equilibrate and remain under 150 C, since those materials are more stable under UV, proton, and electron irradiation.

More sophisticated instrumentation (designed to reveal stress patterns during tensile-property testing) might indicate effects of film temperature excursions during irradiation. Boeing did not employ such instrumentation during this work. We observed no visual differences in the responses or appearances of various portions of samples, neither during irradiation nor during post-irradiation testing. (The only exception being the physical tearing and distortion noted earlier for TOR-LMBP.) Therefore, the extent of sample contact (or lack of it) with its underlying mandrel/substrate probably had no substantial effect, and film temperature excursions during irradiation were probably not great enough to cause fundamental changes in polymer structure or strength. We conclude that the space radiation simulation that we conducted was effective in determining the most stable and least stable films for solar absorptance and tensile strength.

RECOMMENDATIONS

The exposure of one or more, perhaps larger, film samples to a test environment that has been optimized with respect to the UV/charge-particle exposure ratio has been suggested. This environment would allow the UV exposure to achieve a level that coincides with electron and proton fluences reached in the same period. For example, a one-year exposure environment would include approximately 9000 UV hours and the equivalent one-year charge particle fluences.

ACKNOWLEDGMENTS

The authors wish to thank Dr. M. J. Meshishnek for his helpful discussions including the environment depth-dose calculations, and Mr. W. Blackwell for valuable discussions on his preliminary environment definition study.

The authors appreciate the contributions of the following individuals during the course of this program. Loren D. Milliman for scientific data programming, James Beymer for fixture design and CAD support, Douglas Franich for test setup and monitoring, Jerry Hobson and preparation staff

REFERENCES

¹ Fogdall, L. B. and S. S. Cannaday, "Effects of Space Radiation on Thin Polymers and Nonmetallics," Heat Transfer and Thermal Control Systems, Vol. 60, p 290-304, Progress in Astronautics and Aeronautics, ed. L. S. Fletcher, 1978.

² Fogdall, L. B. and S. S. Cannaday, "Space Radiation Effects of a Simulated Venus/Mercury Flyby on Solar Absorptance and Transmittance Properties of Solar Cells, Cover Glasses, Adhesives and Kapton Film." AIAA Paper 71-452, April 1971.

³ Winkler, W., "Material Performance Under Combined Stresses in the Hard Space Environment of the Sun-probe HELIOS-A," Acta Astronautica 10, 189-205 (1983).

⁴ Russell, D.A., L. B. Fogdall, and G. Bohnhoff-Hlavacek, "Simulated Space Environmental Testing on Thin Films," NASA/CR-2000-210101, Final Report for NASA Langley Research Center, April, 2000

⁵ CP-1 and CP-2 manufactured by SRS Technologies.

⁶ TOR-RC and TOR-LMBP manufactured by Triton Systems, Inc.

⁷ Russell, D. A., L. B. Fogdall, and G. Bohnhoff-Hlavacek, "Effects of UV, Protons, and Electrons on Polymer Films for Spacecraft Applications Including NASA Next Generation Space Telescope." Final Report to NASA-Goddard Space Flight Center for Contract S-40584-G, November 2000.

NOTES